Brief report

Recurrent *BRAF* mutations in Langerhans cell histiocytosis

Gayane Badalian-Very,[1-3] Jo-Anne Vergilio,[4,5] Barbara A. Degar,[6-8] Laura E. MacConaill,[9] Barbara Brandner,[1-3] Monica L. Calicchio,[4] Frank C. Kuo,[5,10] Azra H. Ligon,[5,10,11] Kristen E. Stevenson,[12] Sarah M. Kehoe,[9] Levi A. Garraway,[1-3,9,13] William C. Hahn,[1-3,9,13] Matthew Meyerson,[1,2,9,13] Mark D. Fleming,[4,5] and Barrett J. Rollins[1-3]

[1]Department of Medical Oncology, Dana-Farber Cancer Institute, Boston, MA; [2]Department of Medicine, Brigham & Women's Hospital, Boston, MA; [3]Department of Medicine, Harvard Medical School, Boston, MA; [4]Department of Pathology, Children's Hospital Boston, MA; [5]Department of Pathology, Harvard Medical School, Boston, MA; [6]Department of Pediatric Oncology, Dana-Farber Cancer Institute, Boston, MA; [7]Department of Medicine, Children's Hospital Boston, MA; [8]Department of Pediatrics, Harvard Medical School, Boston, MA; [9]Center for Cancer Genome Discovery, Dana-Farber Cancer Institute, Boston, MA; [10]Department of Pathology, Brigham & Women's Hospital, Boston, MA; [11]Center for Molecular Oncologic Pathology, Dana-Farber Cancer Institute, Boston, MA; [12]Department of Biostatistics and Computational Biology, Dana-Farber Cancer Institute, Boston, MA; and [13]Broad Institute of Harvard and Massachusetts Institute of Technology, Cambridge, MA

Langerhans cell histiocytosis (LCH) has a broad spectrum of clinical behaviors; some cases are self-limited, whereas others involve multiple organs and cause significant mortality. Although Langerhans cells in LCH are clonal, their benign morphology and their lack (to date) of reported recurrent genomic abnormalities have suggested that LCH may not be a neoplasm. Here, using 2 orthogonal technologies for detecting cancer-associated mutations in formalin-fixed, paraffin-embedded material, we identified the oncogenic BRAF V600E mutation in 35 of 61 archived specimens (57%). TP53 and MET mutations were also observed in one sample each. BRAF V600E tended to appear in younger patients but was not associated with disease site or stage. Langerhans cells stained for phospho-mitogen–activated protein kinase kinase (phospho-MEK) and phospho-extracellular signal-regulated kinase (phospho-ERK) regardless of mutation status. High prevalence, recurrent *BRAF* mutations in LCH indicate that it is a neoplastic disease that may respond to RAF pathway inhibitors. (*Blood*. 2010;116(11):1919-1923)

Introduction

Langerhans cell histiocytosis (LCH) is a rare proliferative disorder of epidermal antigen-presenting cells.[1,2] It can follow a mild clinical course and even resolve spontaneously,[3,4] but it can also involve multiple organ systems with fatal consequences in 20% of disseminated cases. LCH's etiology is unknown. The benign morphology of its proliferating cells and its characteristic inflammatory infiltrates suggest that LCH may be an inflammatory disorder,[3] and dysregulated expression of inflammatory cytokines, such as interleukin-17A, has been reported.[5] However, the pathologic Langerhans cells (LCs) in LCH are clonal.[6,7] Although clonality is an important feature of neoplasia, recurrent genomic abnormalities would be required to demonstrate that LCH is a neoplasm; and, to date, none has been reported.[8] Therefore, we interrogated LCH tissue samples using a mass spectrometric method that tests for the presence of a large number of cancer-associated mutations in formalin-fixed, paraffin-embedded material.

Methods

Patients and samples

Paraffin blocks archived in the Departments of Pathology at Brigham and Women's Hospital and Children's Hospital Boston were retrieved and diagnoses confirmed. For bone lesions, paraffin blocks containing undecalcified curettings or adjacent soft tissue were used for DNA extraction. Fresh frozen material was retrieved from an LCH case stored at Dana-Farber Cancer Institute. Institutional Review Board approval was obtained for the analysis of anonymized, discarded tissue.

Mass spectrometric genotyping

Blocks were cored in regions of highest histiocyte density, and DNA was extracted using QIAmp DNA FFPE tissue kit (QIAGEN catalog #56404). Multiplexed mass spectrometric genotyping using the OncoMap platform was performed as described in supplemental data (available on the *Blood* Web site; see the Supplemental Materials link at the top of the online article).[9,10] After an initial screen using iPLEX chemistry, which includes 1047 assays interrogating 983 unique mutations across 115 genes (supplemental Tables 6-7), candidate mutations were validated using homogeneous mass extension (hME) chemistry on unamplified genomic DNA.[9]

Pyrosequencing

DNA was amplified using the PyroMark Q24 BRAF kit (QIAGEN). Polymerase chain reaction products were sequenced with 5-CACTCCATCGAGATTTC-3 as a sequencing primer and CTGCATGCATGCA as the dispensation order using the PyroMark MD System (Biotage AB and Biosystems). Samples with mutant allele frequencies less than 4% were considered wild-type; those with frequencies of 4% or greater were considered mutant.

Immunofluorescence

Anti-CD1a (clone MTB1, Ventana Medical Systems) was applied to sections from paraffin blocks followed by Alexa Fluor 488–conjugated goat

Submitted April 8, 2010; accepted May 19, 2010. Prepublished online as *Blood* First Edition paper, June 2, 2010; DOI 10.1182/blood-2010-04-279083.

An Inside *Blood* analysis of this article appears at the front of this issue.

The online version of this article contains a data supplement.

The publication costs of this article were defrayed in part by page charge payment. Therefore, and solely to indicate this fact, this article is hereby marked "advertisement" in accordance with 18 USC section 1734.

Table 1. Mutations in LCH

Patient no.*	Age, y*	Sex*	Disease site*	Stage*	OncoMap†	Pyrosequencing‡
Cohort I						
1	2	M	Bone	Unifocal	BRAF V600E	BRAF V600E (7.84%)
2	6	F	Bone	Unifocal	None	WT (0.00%)
3	NA	NA	Bone	NA	None	WT (1.32%)
4	0.9	F	Lymph node	Multifocal	BRAF V600E	BRAF V600E (15.35%)
5	2	M	Bone	Multifocal	BRAF V600E	BRAF V600E (11.39%)
6	12	M	Bone	Unifocal	None	WT (1.51%)
7	7	M	Bone	Unifocal	None	BRAF V600E (5.52%)‖
8	1.3	M	Lymph node	Multifocal	BRAF V600E	BRAF V600E (25.56%)
9	4	M	Bone	Unifocal	BRAF V600E	NT
10	5	M	Soft tissue	Unifocal	BRAF V600E	BRAF V600E (20.09%)
11	2	M	Bone	Unifocal	BRAF V600E	BRAF V600E (30.87%)
12	1.6	F	Bone	Multifocal	None	WT (0.00%)
13	6	M	Bone	Unifocal	BRAF V600E	BRAF V600E (12.65%)
14	1	M	Bone	Unifocal	None	NT
15	8	M	Bone	Unifocal	None	WT (0.45%)
16	9	F	Bone	Unifocal	BRAF V600E	NT
17	9	M	Bone	Multifocal	None	NT
18	17	M	Bone	Unifocal	BRAF V600E, MET E168D	BRAF V600E (11.06%)
19	11	M	Bone	Unifocal	BRAF V600E	BRAF V600E (18.73%)
20	0.8	F	Bone	Unifocal	BRAF V600E	BRAF V600E (29.91%)
21	17	M	Soft tissue	Unifocal	TP53 R175H	NT
22	7	F	Bone	Unifocal	BRAF V600E	BRAF V600E (4.87%)
23	9	M	Bone	Unifocal	BRAF V600E	BRAF V600E (12.44%)
24	2	M	Bone	Unifocal	None	NT
25	5	F	Skin	Unifocal	BRAF V600E	BRAF V600E (8.94%)
26	27	M	Bone	Unifocal	CUBN I3189V	WT (0.55%)
27	26	M	Bone	NA	BRAF V600E	BRAF V600E (19.80%)
28	43	M	Bone	Unifocal	BRAF V600E	BRAF V600E (26.31%)
29	53	M	Lung	Unifocal	None	NT
30	25	F	Thyroid	Unifocal	None	WT (2.01%)
31	47	F	Bone	Unifocal	None	WT (0.63%)
32	31	F	Bone	Multifocal	None§	WT (0.45%)
33	51	F	Lung	Unifocal	None	NT
34	48	F	Thymus	Unifocal	None	NT
35	35	M	Bone	NA	Insufficient DNA	WT (0.26%)
Cohort II						
36	8	M	Bone	NA	BRAF V600E	BRAF V600E (17.02%)
37	40	M	Bone	Unifocal	None	NT
38	42	M	Bone	Unifocal	BRAF V600E	BRAF V600E (41.98%)
39	51	M	Lung	Unifocal	BRAF V600E	BRAF V600E (10.87%)
40	54	M	Lung	NA	None	WT (1.50%)
41	10	F	Soft tissue	Multifocal	None	WT (0.00%)
42	11	M	Bone	Unifocal	None	NT
43	61	M	Lung	Unifocal	None	WT (0.60%)
44	24	F	NA	Unifocal	Insufficient DNA	NT
45	40	M	Bone	Unifocal	None	WT (0.28%)
46	48	F	Lung	Unifocal	None	NT
47	16	M	Skin	Unifocal	Insufficient DNA	NT
48	59	F	Lung	Unifocal	BRAF V600E	BRAF V600E (10.54%)
49	1.6	F	Mediastinum	Unifocal	BRAF V600E	NT
50	4	F	Bone	Unifocal	BRAF V600E	BRAF V600E (25.79%)
51	38	F	Lung	Unifocal	None	WT (0.64%)
52	1.3	M	LN	Multifocal	BRAF V600E	BRAF V600E (27.49%)

NT indicates not tested (because of insufficient DNA for analysis); NA, not applicable; BRAF, B-Raf; MET, c-met proto-oncogene; TP53, p53 tumor suppressor gene; KRAS, K-Ras; CUBN, cubilin (intrinsic factor-cobalamin receptor); and None, none of the 983 mutant alleles measured by OncoMap was detected or was validated after detection during initial iPLEX screening.

*Cohort I and Cohort II are composed of separately retrieved batches of archived patient material. Frozen indicates a fresh frozen LCH sample for which no clinical information was available.

†Validated mutations identified by OncoMap mass spectrometric genotyping. Amino acid changes produced by specific mutations are indicated using standard designations.

‡*BRAF* allele status based on mutant allele abundance determined by pyrosequencing. The percentage of mutant alleles detected in each sample is shown in parentheses. BRAF V600E status was called on samples in which mutant sequences represented $>$ 4% of total *BRAF* sequences ("Methods").

§Sample failed genotyping on hME analysis, but no mutations were detected on iPLEX analysis.

‖Because the pyrosequencing test is a clinically validated test performed in a Clinical Laboratory Improvement Amendment-certified laboratory, sample number 7 was assigned mutant BRAF V600E status.

Table 1. Mutations in LCH (continued)

Patient no.*	Age, y*	Sex*	Disease site*	Stage*	OncoMap†	Pyrosequencing‡
53	3	M	Bone	Unifocal	BRAF V600E	BRAF V600E (26.66%)
54	59	F	Lung	Unifocal	BRAF V600E	NT
55	13	M	Bone	Unifocal	BRAF V600E	BRAF V600E (24.19%)
56	56	M	Lung	Unifocal	BRAF V600E	NT
57	16	M	Bone	Unifocal	BRAF V600E	BRAF V600E (15.80%)
58	20	F	Soft tissue	Unifocal	BRAF V600E	NT
59	12	M	Bone	Unifocal	BRAF V600E	BRAF V600E (35.57%)
60	61	M	Lung	Unifocal	BRAF V600E	BRAF V600E (12.91%)
61	43	M	Bone	Unifocal	BRAF V600E	BRAF V600E (17.33%)
62	51	F	Lung	Unifocal	None	WT (1.94%)
Frozen						
63	NA	NA	NA	NA	Not performed	BRAF V600E (9.17%)

NT indicates not tested (because of insufficient DNA for analysis); NA, not applicable; BRAF, B-Raf; MET, c-met proto-oncogene; TP53, p53 tumor suppressor gene; KRAS, K-Ras; CUBN, cubilin (intrinsic factor-cobalamin receptor); and None, none of the 983 mutant alleles measured by OncoMap was detected or was validated after detection during initial iPLEX screening.

*Cohort I and Cohort II are composed of separately retrieved batches of archived patient material. Frozen indicates a fresh frozen LCH sample for which no clinical information was available.

†Validated mutations identified by OncoMap mass spectrometric genotyping. Amino acid changes produced by specific mutations are indicated using standard designations.

‡*BRAF* allele status based on mutant allele abundance determined by pyrosequencing. The percentage of mutant alleles detected in each sample is shown in parentheses. BRAF V600E status was called on samples in which mutant sequences represented > 4% of total *BRAF* sequences ("Methods").

§Sample failed genotyping on hME analysis, but no mutations were detected on iPLEX analysis.

‖Because the pyrosequencing test is a clinically validated test performed in a Clinical Laboratory Improvement Amendment-certified laboratory, sample number 7 was assigned mutant BRAF V600E status.

anti–mouse immunoglobulin G (IgG) $F(ab')_2$ fragments (Cell Signaling Technologies). Then, antiphospho-mitogen–activated protein kinase kinase (MEK) or antiphospho-extracellular signal-regulated kinase (ERK) antibodies (rabbit IgG from Cell Signaling Technologies) were applied followed by Alexa Fluor 555–conjugated goat anti–rabbit IgG $F(ab')_2$ fragments (Cell Signaling Technologies). Nuclei were counterstained using 4,6-diamidino-2-phenylindole (DAPI; Vector Laboratories). Controls using class- or subclass-matched nonspecific immunoglobulins showed no specific staining.

Statistical analysis

Fisher exact test was performed for categorical comparisons, and the Wilcoxon rank-sum test was performed for 2-sample comparison of continuous measures. A Pearson correlation coefficient (r) test was used to determine the relationship between 2 continuous measures. All tests were 2-sided and considered significant at the .05 level. Unadjusted and adjusted exact logistic regression models were also constructed to test for an association between the BRAF V600E mutation and clinical characteristics.

Results and discussion

To test for cancer-related mutations in LCH, we retrieved 35 paraffin blocks from the pathology archives of our hospitals (Cohort I). DNA extracted from LCH-enriched cores was analyzed for the presence of cancer-related mutations using OncoMap, a mass spectrometric method of allele detection optimized for formalin-fixed, paraffin-embedded material.[9,10] BRAF V600E was identified in 17 of 34 evaluable samples (one case yielded insufficient DNA for analysis; Table 1). Other validated mutations included MET E168D and TP53 R175H in one case each. A second set of 27 samples was independently retrieved and analyzed (Cohort II). Two had insufficient DNA for analysis, but BRAF V600E was found in 16 of the remaining 25.

To confirm the presence of BRAF V600E using an orthogonal technology, 44 samples were pyrosequenced (insufficient material remained to sequence all samples; Table 1). Results were consistent with OncoMap, except for 2 cases: one in which pyrosequencing detected wild-type alleles in a sample with insufficient DNA for OncoMap and one in which pyrosequencing detected BRAF V600E in a sample called wild-type by OncoMap. Because our pyrosequencing assay is a clinically validated test executed in a laboratory certified pursuant to the Clinical Laboratory Improvement Amendment, we assigned mutant status to this sample. Finally, pyrosequencing detected BRAF V600E in a freshly frozen LCH sample, suggesting that the mutation is not an artifact of fixation technique (Table 1). Overall, BRAF V600E was present in 35 of 61 evaluable cases for a mutation frequency of 57%. As controls, we examined 5 cases of dermatopathic lymphadenopathy, a reactive proliferative disease that includes an LC component, and 4 cases of Rosai-Dorfman disease, a histiocytic disorder of macrophage lineage. No *BRAF* mutations were detected in these samples (supplemental Table 1).

The median age of patients who carried the mutation was less than that of patients who did not ($P = .03$, supplemental Table 2); age was also associated with mutation status in the unadjusted exact logistic model ($P = .04$) but not in the adjusted exact logistic model ($P = .09$) (supplemental Table 3). No other available clinical characteristics correlated with the presence of BRAF V600E, including disease site or stage. Our incomplete clinical dataset precludes drawing any inferences about the effect of mutation status on clinical outcomes.

Three indirect criteria indicated that the mutant *BRAF* alleles were specifically in LCs. First, the proportion of *BRAF* mutant alleles determined by pyrosequencing was 3-fold to 21-fold higher in LC-enriched material obtained by laser-capture microdissection compared with LC-depleted material (supplemental Table 4). Second, the abundance of mutant *BRAF* alleles in each sample correlated with the percentage of LCs in those samples ($r = 0.68$, $P < .001$, supplemental Figure 1). The proportion of mutant alleles was approximately half the proportion of LCs in the samples, suggesting that the mutation was present in a single heterozygous copy, although this is speculative. Third, LCs specifically stained for phospho-MEK and phospho-ERK (Figure 1), indicating activation of the BRAF signaling cascade in those cells. The intensity of

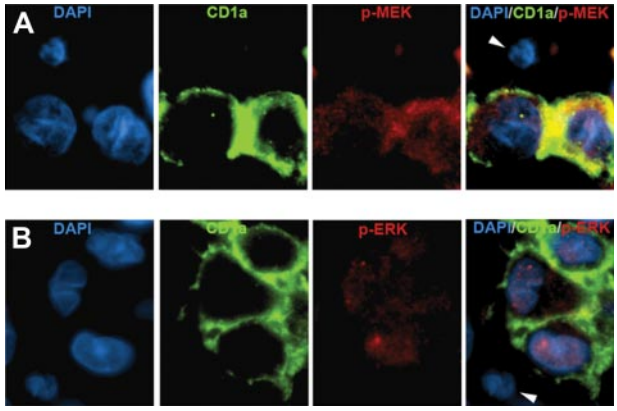

Figure 1. Immunofluorescence analysis of BRAF pathway activation in LCH. (A) LCH sample stained with DAPI (blue), anti-CD1a (green), antiphospho-MEK (red), and a merged image of all 3 stains. (B) LCH sample stained with DAPI (blue), anti-CD1a (green), antiphospho-ERK (red), and a merged image of all 3 stains. Arrowheads indicate CD1a-negative cells that are also negative for phospho-MEK and phospho-ERK. (Technical details described in supplemental Methods.)

phospho-MEK and phospho-ERK staining by immunohistochemistry (supplemental Figure 2) did not vary with *BRAF* mutational status (supplemental Table 5), suggesting that BRAF pathway activation may occur generally in LCH but that *BRAF* mutation is not its only cause. *BRAF* gene duplication has been associated with pathway activation in pediatric low-grade astrocytomas,[11,12] but we detected no gene duplication by fluorescence in situ hybridization (FISH) in 43 analyzable samples.

The presence of BRAF V600E in 57% of archived LCH specimens from 2 independent institutions strongly suggests that LCH is a neoplasm. This finding adds LCH to a growing list of neoplastic diseases in which the transformed cell harbors this mutation.[13,14] BRAF V600E is also present in benign nevi, and this has been cited as an example of oncogene-induced senescence in vivo.[15] A similar mechanism may underlie examples of spontaneous remission in LCH as well as the frequent appearance of overexpressed wild-type p53.[8,16] The presence of BRAF V600E in pulmonary LCH was surprising considering the fact that 70% of these lesions have been reported to be nonclonal.[17] We speculate that, in susceptible persons, cigarette smoke may generate the transversion that characterizes this allele. This would result in multiple transformed clones throughout the lung that, in the aggregate, produce polyclonal disease with the same mutation in all of the clones. A similar situation has been described in nevi.[18]

As with nevi, of course, additional genetic changes may be required in order for LCs harboring BRAF V600E to progress to LCH. Although OncoMap tests a large number of alleles, it is not exhaustive, and additional abnormalities not measured by this test may yet be discovered in LCH. Nonetheless, specific inhibition of BRAF signaling is effective in blocking the proliferation of melanoma cells that have additional genomic abnormalities.[19,20] A similar approach may also produce responses in patients with LCH.

Acknowledgments

The authors thank Matt Davis and Charlie Hatton for OncoMap technical support, the Center for Advanced Molecular Diagnostics at Brigham & Women's Hospital for pyrosequencing, Natalie Vena for FISH analysis technical support, Dr Stephen Sallan for encouraging the LCH research program, and Dr Phillip Kantoff for his help.

This work was supported in part by the Histiocytosis Association of America, Team Ippolittle/Deloitte of the Boston Marathon Jimmy Fund Walk, the Mufson family, and a US Public Health Service grant (AI050225). The Pathology Specimen Locator Core is supported by a National Cancer Institute Cancer Center Support Grant (P30 CA06516) to the Dana-Farber/Harvard Cancer Center.

Authorship

Contribution: G.B.-V. obtained tissue cores, performed laser-capture microdissection, isolated DNA, performed immunofluorescence, and analyzed immunohistochemistry; J.-A.V. conducted pathology evaluation and analyzed immunohistochemistry; B.A.D. evaluated clinical characteristics for each case; B.B. initiated tissue and DNA acquisition for OncoMap; M.L.C. performed immunohistochemistry; F.C.K. performed pyrosequencing; A.H.L. performed FISH; K.E.S. performed statistical analyses; S.M.K. performed OncoMap analysis; L.E.M. performed and interpreted OncoMap analysis; L.A.G. performed and oversaw OncoMap analysis; W.C.H. and M.M. evaluated and oversaw OncoMap analysis; M.D.F. reviewed all pathology diagnoses and immunohistochemistry and identified appropriate control cases; and B.J.R. conceived and coordinated the genotyping project.

Conflict-of-interest disclosure: The authors declare no competing financial interests.

Correspondence: Barrett J. Rollins, Department of Medical Oncology, Dana-Farber Cancer Institute, 44 Binney St, Boston, MA 02115; e-mail: barrett_rollins@dfci.harvard.edu.

References

1. Bechan GI, Egeler RM, Arceci RJ. Biology of Langerhans cells and Langerhans cell histiocytosis. *Int Rev Cytol.* 2006;254:1-43.
2. Filipovich A, McClain K, Grom A. Histiocytic disorders: recent insights into pathophysiology and practical guidelines. *Biol Blood Marrow Transplant.* 2010;16(1)[suppl]: S82-S89.
3. Broadbent V, Pritchard J, Davies EG, et al. Spontaneous remission of multi-system histiocytosis X. *Lancet.* 1984;1(8371):253-254.
4. McElligott J, McMichael A, Sangueza OP, Anthony E, Rose D, McLean TW. Spontaneous regression of langerhans cell histiocytosis in a neonate with multiple bony lesions. *J Pediatr Hematol Oncol.* 2008;30(1):85-86.
5. Coury F, Annels N, Rivollier A, et al. Langerhans cell histiocytosis reveals a new IL-17A-dependent pathway of dendritic cell fusion. *Nat Med.* 2008; 14(1):81-87.
6. Willman CL, Busque L, Griffith BB, et al. Langerhans'-cell histiocytosis (histiocytosis X): a clonal proliferative disease. *N Engl J Med.* 1994;331(3): 154-160.
7. Yu RC, Chu C, Buluwela L, Chu AC. Clonal proliferation of Langerhans cells in Langerhans cell histiocytosis. *Lancet.* 1994;343(8900):767-768.
8. da Costa CE, Szuhai K, van Eijk R, et al. No genomic aberrations in Langerhans cell histiocytosis as assessed by diverse molecular technologies. *Genes Chromosomes Cancer.* 2009;48(3): 239-249.
9. MacConaill LE, Campbell CD, Kehoe SM, et al. Profiling critical cancer gene mutations in clinical tumor samples. *PLoS ONE.* 2009;4(11):e7887.
10. Thomas RK, Baker AC, Debiasi RM, et al. High-throughput oncogene mutation profiling in human cancer. *Nat Genet.* 2007;39(3):347-351.
11. Jones DT, Kocialkowski S, Liu L, et al. Tandem duplication producing a novel oncogenic BRAF fusion gene defines the majority of pilocytic astrocytomas. *Cancer Res.* 2008;68(21):8673-8677.
12. Pfister S, Janzarik WG, Remke M, et al. BRAF gene duplication constitutes a mechanism of MAPK pathway activation in low-grade astrocytomas. *J Clin Invest.* 2008;118(5):1739-1749.
13. Davies H, Bignell GR, Cox C, et al. Mutations of the BRAF gene in human cancer. *Nature.* 2002; 417(6892):949-954.
14. Michaloglou C, Vredeveld LC, Mooi WJ, Peeper

DS. BRAF(E600) in benign and malignant human tumours. *Oncogene.* 2008;27(7):877-895.

15. Michaloglou C, Vredeveld LC, Soengas MS, et al. BRAFE600-associated senescence-like cell cycle arrest of human naevi. *Nature.* 2005;436(7051): 720-724.
16. Weintraub M, Bhatia KG, Chandra RS, Magrath IT, Ladisch S. p53 expression in Langerhans cell histiocytosis. *J Pediatr Hematol Oncol.* 1998; 20(1):12-17.
17. Yousem SA, Colby TV, Chen YY, Chen WG, Weiss LM. Pulmonary Langerhans' cell histiocytosis: molecular analysis of clonality. *Am J Surg Pathol.* 2001;25(5):630-636.
18. Lin J, Takata M, Murata H, et al. Polyclonality of BRAF mutations in acquired melanocytic nevi. *J Natl Cancer Inst.* 2009;101(20): 1423-1427.
19. Hingorani SR, Jacobetz MA, Robertson GP, Herlyn M, Tuveson DA. Suppression of BRAF(V599E) in human melanoma abrogates transformation. *Cancer Res.* 2003;63(17):5198-5202.
20. Hoeflich KP, Herter S, Tien J, et al. Antitumor efficacy of the novel RAF inhibitor GDC-0879 is predicted by BRAFV600E mutational status and sustained extracellular signal-regulated kinase/mitogen-activated protein kinase pathway suppression. *Cancer Res.* 2009;69(7):3042-3051.